# Epitaxial Crystal Growth and Solid-State Polymerization of Piperonyl Muconate on the {001} Surface of KCl Crystal for Controlling Polymer Chain Alignment

Katsuya Onodera, Chiaki Tanioku, and Akikazu Matsumoto*

Department of Applied Chemistry and Bioengineering, Graduate School of Engineering, Osaka City University, Sugimoto, Sumiyoshi-ku, Osaka 558-8585, Japan

ABSTRACT: We investigated the crystal growth of piperonyl (E,E)-muconate [bis(3,4-methylenedioxybenzyl) (E,E)-muconate, MDO] on inorganic crystalline substrates during vapor deposition for the control of polymer chain alignment by the subsequent solid-state photopolymerization of the MDO monomer thin films deposited on the substrate. We controlled the arrangement of the MDO molecules and the polymer chains produced on the substrate, depending on the lattice parameters of the substrate surfaces used. The epitaxial crystal growth of MDO on the {001} plane of a KCl single crystal was observed under the condition that the crystal lattice lengths of MDO agreed well with the specific space distance of the substrate; i.e., the KCl cubic crystal resulted in a d_{110} value of 4.45 Å, which was very close to the value of the monomer stacking distance in the MDO crystal (d_s = 4.43 Å). On the other hand, slightly large and too small d_{110} values for KBr and NaCl, respectively, resulted in the less controlled and no epitaxial crystal growth of MDO. The irradiation of polarized UV light on the MDO thin-film crystal produced highly regulated polymer alignment in a specific direction on the KCl substrate.

KEYWORDS: controlled radical polymerization, crystal engineering, muconic ester, photopolymerization, thin-film crystals, topochemical reaction, X-ray crystal structure analysis
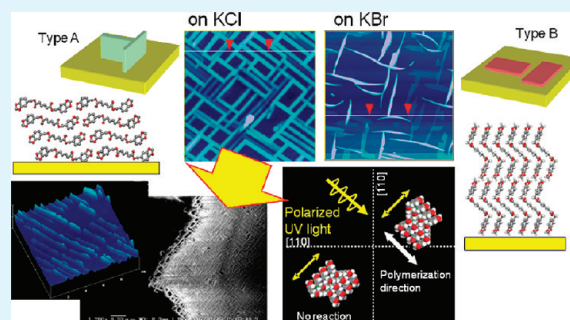
INTRODUCTION

The precise control of the primary structures of polymer chains attracts great interest in the polymer synthetic field and material sciences; for example, the control of molecular weight, molecular weight distribution, chain-end functionality, branching and grafting structures, tacticity, and repeating unit sequences such as block, alternating, and sequential copolymer syntheses.[1−6] The topochemical polymerization of diacetylene,[7−15] diene,[16−20] and other monomers[21−25] is a unique method for the in-situ fabrication of crystalline polymer materials with a highly controlled structure. We previously reported the topochemical polymerization of various derivatives of muconic and sorbic acids as the 1,3-diene monomers in the solid state under UV, X-ray, and γ-ray irradiation or upon heating.[17−20] There are several possible reaction pathways during the solid-state photoreaction of the muconates, such as topochemical polymerization,[26−32] [2+2] cyclodimerization,[33−35] and EZ-isomerization,[36−39] but one of these reactions exclusively occurs depending on the molecular stacking structure in the crystals.[40] During the topochemical polymerization, the polymerization reactivity is strictly determined by the monomer crystal structure. For example, the stacking distance (d_s) of the monomers should be close to 5 Å for the process of topochemical polymerization.[41,42] The reactivity and the structure of the products during topochemical reactions are predictable based on the crystal structure of a reactant,[43−45] but

the control of crystal growth is still limited, for example, the crystal growth rate, the shape and habit of the crystals, and polymorphs.

The selective and controlled modification of substrate surfaces using functional polymer materials is useful for the fabrication of electronic and other devices.[46−53] Here we describe the controlled crystal growth of diene monomer molecules on an inorganic substrate by vapor deposition in order to align the polymer chains, which are produced during the solid-state polymerization of the deposited monomer crystals. In this study, we used piperonyl (E,E)-muconate, i.e., bis(3,4-methylenedioxybenzyl) (E,E)-muconate (MDO) as the monomer (Scheme 1) due to the following advantageous characteristics. The MDO monomer is readily synthesized with muconic acid and a commercial alcohol,[54,55] and no polymorph has been found in our laboratory in the recent decade. The solid-state polymerization of MDO moderately occurs under UV irradiation.[42] No EZ-photoisomerization occurs under UV irradiation in the solid state, and thermal polymerization hardly occurs in the dark. These characteristics are suitable for easy handling during thin-film crystal fabrication by vapor deposition. Furthermore, the single crystal structure of MDO

Scheme 1
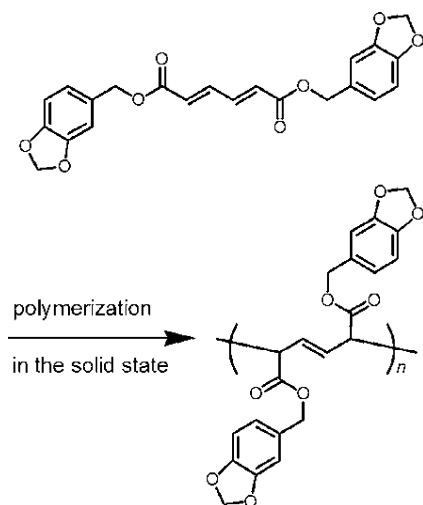
is already known by an X-ray structure analysis.[42] We used the {001} plane of KCl, KBr, and NaCl crystals as the substrate for the crystal growth of MDO, because of a facile cleavage procedure for the preparation of a clean and determined face of the single crystals. We investigated the structures of the MDO crystals deposited on the specific surface of the inorganic substrates by atomic force microscopy (AFM) and wide-angle X-ray diffraction (XRD) measurements. The polymer thin films were obtained during the photopolymerization under UV irradiation in the solid state. The selective polymerization using polarized UV light was also carried out to control the alignment of the polymer chains on the substrate.

EXPERIMENTAL SECTION

General Procedures. The FT-IR spectra were recorded using a JASCO FT/IR 430 spectrometer equipped with a JASCO Intron IRT-30 infrared microscope. The AFM images were observed in the tapping mode using a NanoScope IIIa SPM system (Digital Instruments-Veeco) equipped with an MMAFM-type multimode SPM unit and an Olympus cantilever OMCL-AC240TS-C2 (resonant frequency 73.4-77.6 Hz, spring constant 2.1-2.5 N/m). The X-ray diffraction profile was recorded on a Rigaku RINT-2100 with monochromatized Cu K$_\alpha$ radiation (1.54184 Å, 40 kV, 40 mA, scan speed 2.0°/min, scan angle 2-40°), equipped with a high-resolution parallel-beam optics system consisting of a parallel slip analyzer PSA100U and a graded multiplayer 2960C1. The scanning electron microscopy (SEM) observation was carried out using Keyence VE-7800 with the accelerating voltage source of 1.5 kV. Photo-polymerization was carried out at the distance of 1 cm using a low-pressure Hg lamp (As One SLUV-4, 365 nm) at room temperature. A polarizer JASCO FDP-203 was used for the irradiation of polarized UV light. We determined the polarized direction of the UV light using the specific cleavage plane of the substrate edge as the standard.

Vapor Deposition. Commercial optical single crystals of KCl, KBr, and NaCl (GL Science, optical cell grade for IR spectroscopy, 35 mm × 35 mm × 5 mm) were used as the substrates for vapor deposition after cubic cleavage on their {001} planes. Vapor deposition was carried out using an Ulvac VPC-410 equipped with a quartz crystal microbalance (QCM) controller CRTM-6000 for monitoring the deposition rate at 1.0×10^{-4} Pa and room temperature without temperature control of the substrates. The static contact angles of the glass plate surfaces were measured using 1 μL of deionized water at room temperature with a Keyence digital microscope VHX-500, and an average value of five measurements at different positions was used. The cleansing of the glass plate was carried out as follows. A glass plate was immersed in acetone with

ultrasonic cleaning twice for 15 min, followed by a similar procedure using 2-propanol. The plate was further subjected to UV ozone cleaning for a determined time before surface modification. The alkylation of the glass plate surface was carried out using a silane coupling agent (5 μL) in 50 mL of chloroform at room temperature for a determined time.

Materials. MDO was synthesized by the previously reported method.[54,55] To (E,E)-muconic acid (0.12 g) in 2 mL of N-methylpyrrolidone in a 10-mL flask equipped with a calcium chloride tube, were added piperonyl bromide (0.33 g) and potassium carbonate (0.27 g), and the solution was stirred in the dark at room temperature for 1 day. The piperonyl bromide was synthesized with a commercial piperonyl alcohol (Tokyo Chemical Industry Co., Ltd.) according to the method reported in the literature.[56] The reaction mixture was poured into 100 mL of water, and the precipitated white solid was filtered and dried under reduced pressure. Pure and platelet MDO crystals were obtained by recrystallization from chloroform. Yield 0.19 g (54%). Mp 145.5−146 °C.

Commercial silane coupling agents, trichlorooctadecylsilane, methyltrimethoxysilane, dimethyldimethoxysilane, and trimethylmethoxysilane (Tokyo Chemical Industry Co., Ltd.) were used without further purification. Solvents were distilled before use.

RESULTS AND DISCUSSION

Crystal Structure of MDO. The monomer and polymer stacking structures in the MDO crystals, which are viewed along the crystallographic a-axis, are shown in Figure 1. In our
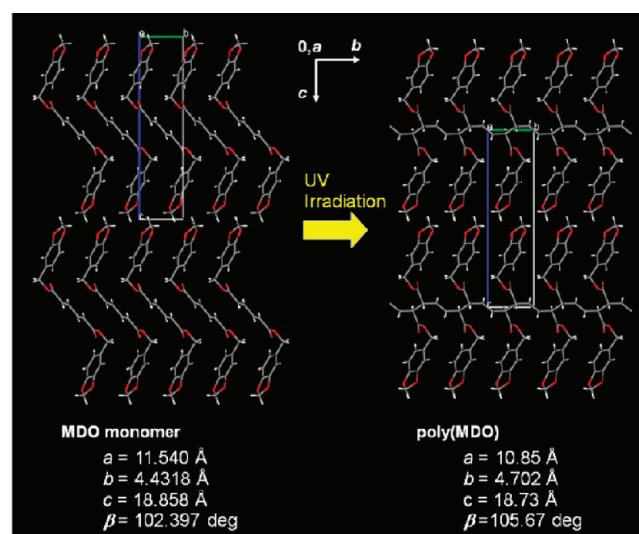

Figure 1. Crystal structures of the MDO monomer and poly(MDO).

previous study,[42] it was revealed that the change in the lattice parameters for MDO was small during polymerization, resulting in the successful formation of polymer single crystals with a high quality appropriate for an X-ray single-crystal structure analysis. The MDO monomer molecules are arranged to form a columnar structure along the b-axis with a d_s value of 4.43 Å. This distance is quite identical to an appropriate value for obtaining the topochemical polymerization of 1,3-diene monomers (4.4−5.2 Å). A repeating distance in the corresponding polymer chains (fiber period) is 4.70 Å, being slightly greater than the d_s value of the MDO monomer. As a result, the lattice length increases along the fiber axis (b-axis) during the polymerization (expansion-type polymerization).[42] Simultaneously, shrinking occurs along the other two axes during the polymerization; 11.54 to 10.85 Å for the a-axis and 18.86 to 18.73 Å for the c-axis.
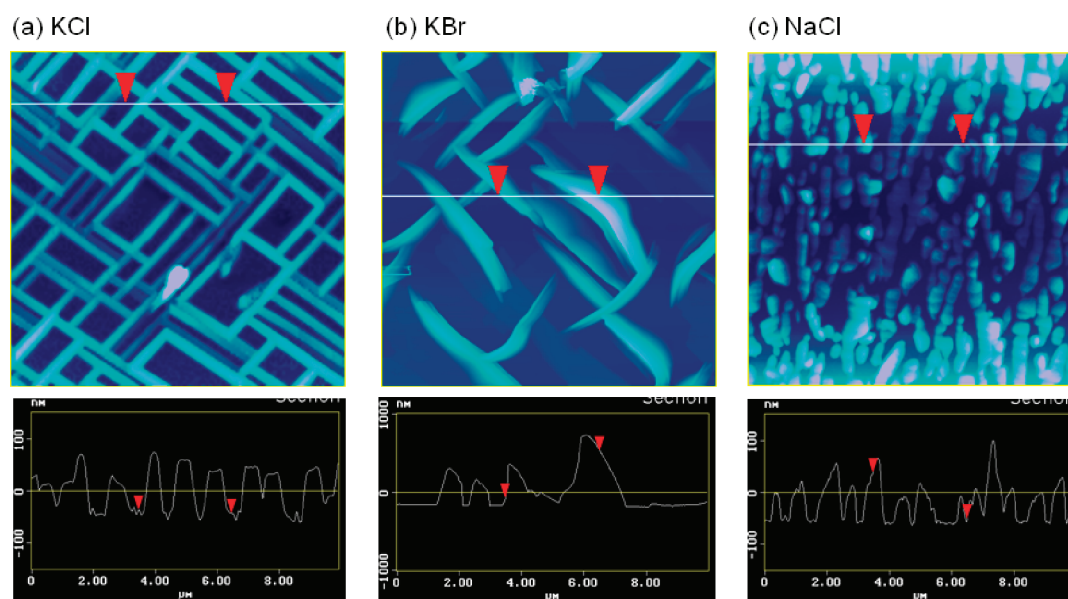
Figure 2. AFM images of the thin-film crystals of MDO fabricated by vapor deposition on the {001} plane of various single-crystal substrates at room temperature. Area 10 μm × 10 μm. (a) KCl, (b) KBr, and (c) NaCl. Deposition rate 0.02 nm/s, deposition time 90 min.
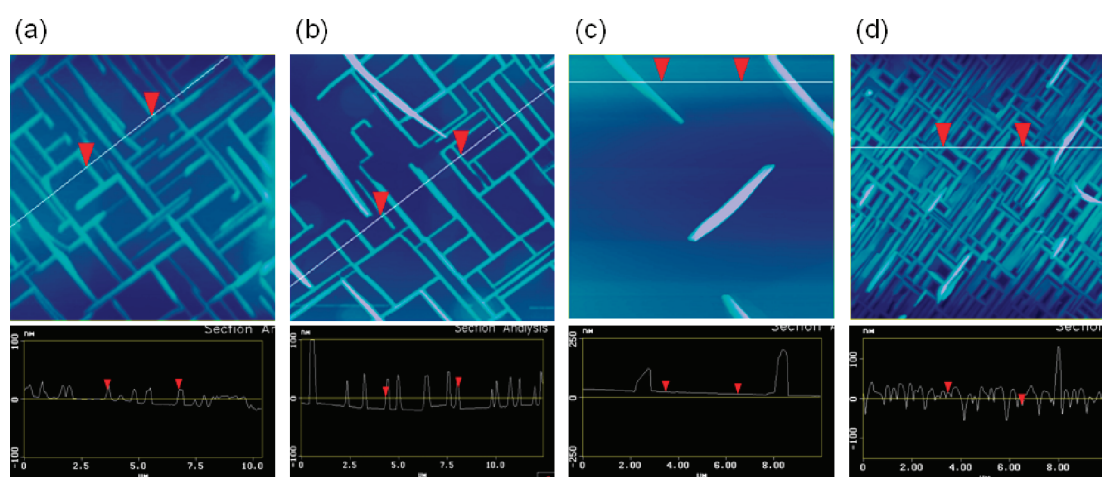

Figure 3. AFM images of the thin-film crystals of MDO fabricated by vapor deposition on the {001} plane of KCl at room temperature under various deposition conditions. Area 10 μm × 10 μm. (a) Deposition rate 0.02 nm/s, deposition time 10 min; (b) deposition rate 0.02 nm/s, deposition time 60 min; (c) deposition rate 0.01 nm/s, deposition time 90 min; and (d) deposition rate 0.15 nm/s, deposition time 90 min.

We fabricated the thin films of the MDO monomer by vapor deposition using the {001} plane of each substrate, i.e., the KCl, KBr, and NaCl single crystals, under high vacuum (1.0×10^{-4} Pa) at room temperature. Figure 2 shows the AFM images of the MDO crystals deposited on various substrates. Thin crystals grew in two orthogonal directions at a right angle on the KCl substrate. Long crystals with a flat top were formed, and the distribution in the width and height of each crystal was small. Similar crystal growth in cross-directions was also observed on KBr, but the shape of the deposited crystals was non-regulated and some crystals were bent. The width and the shape of the crystals deposited on KBr were not uniform, being different from the features of the crystals deposited on KCl. The MDO deposited on NaCl was crystalline, but no anisotropic crystal growth occurred, i.e., a polycrystalline thin film was formed on NaCl. During the crystal growth on KCl, the number and size of the deposited crystals depended on the deposition rate and time. The crystal thickness increased with an increase in the deposition time, as shown in Figure 3, whereas the crystal

length and width retained approximately constant values. On the other hand, the deposition rate changed the number of the formed crystals due to a change in the frequency of nucleation for the crystal growth on the substrate surface. For further experiments in this study, the deposition was carried out at the rate of 0.02 nm/s.

Photopolymerization of MDO. The polymerization of the MDO deposited on the substrates was carried out under UV irradiation. The process of polymerization was confirmed by a change in the absorption band due to the C=O vibration stretching for the conjugated carbonyl group observed at 1714 cm^{-1} to the non-conjugated one at 1726 cm^{-1} in the IR spectrum (Figure 4). The polymerization of the MDO thin-film crystals in this study was completed within 30-min irradiation of UV light due to a high efficiency of the homogeneous photoirradiation of the whole sample, the thickness of which was less than 100 nm, whereas the photoreaction of large-size bulk crystals often starts from their surface and hardly occurs in the inner part.
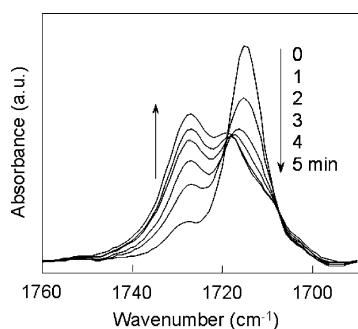
Figure 4. Change in the carbonyl absorption band in the IR spectrum of the MDO crystals deposited on KCl during photoirradiation using a high-pressure UV lamp (365 nm).

After the photopolymerization, the produced polymer film was immersed in chloroform in order to remove trace amounts of the remaining monomer. The isolated poly(MDO) with a crosshatched structure was flexible and partly fibrous, as shown in the SEM images in Figure 5. We have determined that the
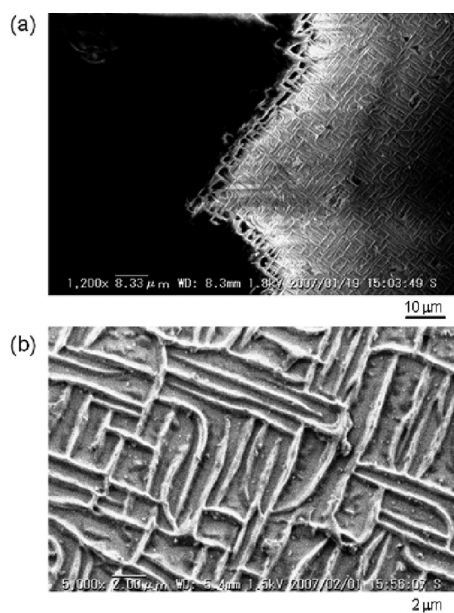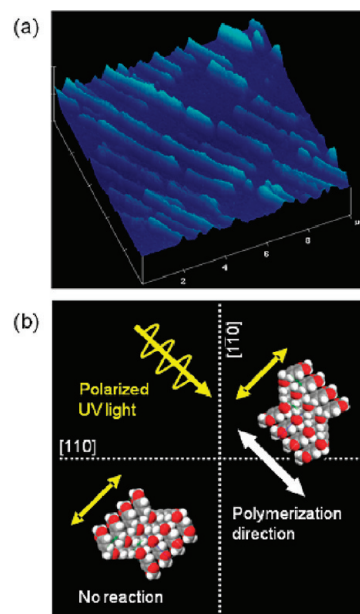

Figure 5. (a) SEM image of poly(MDO) thin film with a crosshatched structure, prepared by the deposition of the MDO monomer on KCl and subsequent polymerization under UV irradiation. The KCl substrate was partly removed at the edge of the thin film. (b) Expanded image of the poly(MDO) thin film.

polymer chains are aligned along the long axis of the crystals, based on the fibrous structure and cracks formed during the polymerization.[26] Interestingly, we can see the fact that some polymeric fibers show a right-angled turn in the crosshatched pattern, as shown in the expanded SEM image (Figure 5b). This suggests that the solid-state polymerization continuously occurs through T- or L-shaped junctions in the crosshatched crystals, and crystallographic phase matches at the boundary of the independent crystals with orthogonally different alignments.

Furthermore, we tried to selectively polymerize the crystals aligned in the same direction using polarized UV light among orthogonally different arrangement of the MDO crystals on KCl. When the polarized light was irradiated on the sample in a direction identical to the crosshatched pattern of the MDO

crystals, the selective polymerization was induced. The AFM image of the isolated poly(MDO) is shown in Figure 6, in


Figure 6. (a) AFM image of poly(MDO) thin films with polymer-chain alignment, prepared by selective photopolymerization under the irradiation of polarized UV light and the removal of the unreacted monomers after polymerization. Substrate KCl, area 10 μm × 10 μm. (b) A schematic model for selective polymerization of MDO deposited on the {001} plane of KCl using polarized UV light.

which the polymer crystals were obtained by dissolving the unreacted monomer with chloroform after photopolymerization. Figure 6b shows a schematic model for the selective induction of the MDO polymerization by the irradiation of polarized UV light and the polymer formation with controlled alignment in a single direction on the substrate.

Epitaxial Crystal Growth Mechanism. We investigated the detailed structure of molecular arrangement in the thin-film crystals by an X-ray diffraction measurement. The crystalline structure of the MDO thin-film crystals obtained in this study was determined to be the same as the previously reported structure[42] for the bulk crystals of MDO, independent of the crystal growth conditions of epitaxial growth by vapor deposition and slow crystallization from a solution, by XRD measurements using crushed powdery samples. As shown in Figure 7, a diffraction line was uniquely observed at $2\theta = 16.7°$ in the XRD profile of the thin-film crystals deposited on KCl. This was assigned as the (20−2) plane of the MDO crystals, based on the calculated diffraction profile for the powder samples (Table 1) using the reported X-ray single crystal structural data.[42] The diffraction of the (40−4) plane was not detected due to very weak intensity. This X-ray diffraction result shows that the MDO molecules are arranged in contact with their side edge (edge-on-stacking) on the KCl substrate, as shown in Figure 7b. In this crystal, the b-axis, which is the identical to the direction of the monomer stacking for polymerization (i.e., the polymer fiber axis), exists in parallel to the substrate surface. The crystal growth rate along the b-axis is greater than the growing rates of the other crystal planes, leading to an elongated crystal growth.

On the other hand, a different X-ray diffraction pattern was observed from the crystals deposited on KBr, as shown in
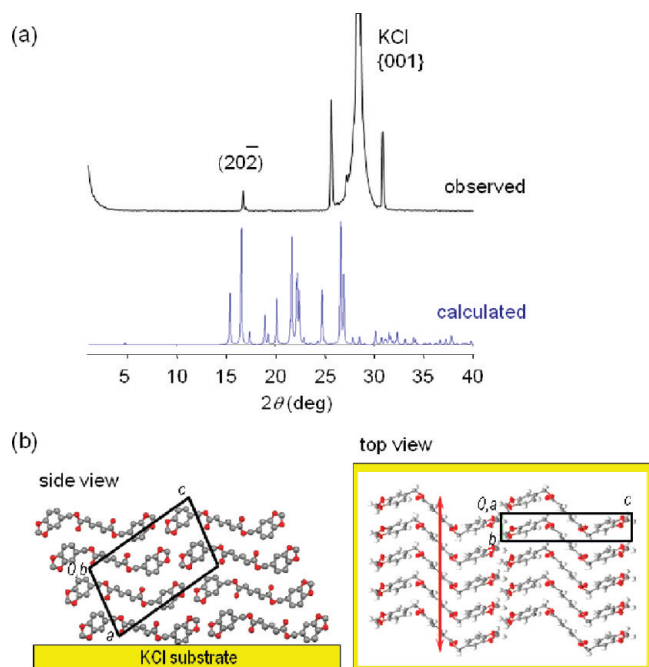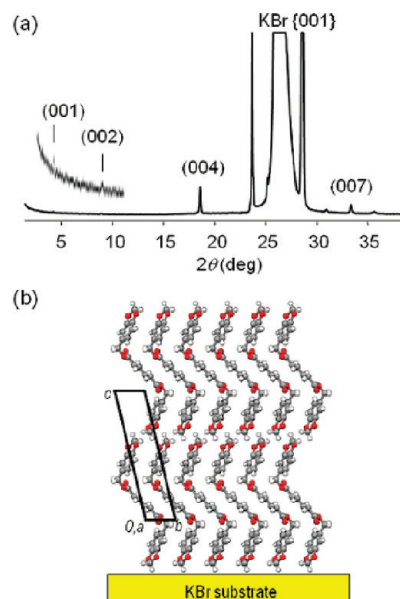
Figure 7. (a) Observed XRD profile of the MDO thin-film crystals deposited on KCl and calculated one based on data for the X-ray single-crystal structure. (b) Edge-on-stacking structure of MDO on KCl.

Table 1. Observed and Calculated 2θ Values for the (hkl) Planes of the MDO Crystals

| Substrate	plane (hkl)	2θ obsd (deg)	2θ calcd (deg)	intensity (calcd) (relative)
KCl	(20-2)	16.70	16.577	98.4
	(40-4)	not detected	33.157	0.5
KBr	(001)	4.807	4.798	1.3
	(002)	9.581	9.596	0.2
	(003)	not detected	14.416	<0.1
	(004)	19.28 (19.39)[a]	19.260 (19.678)[b]	9.7
	(005)	not detected	24.143	0.7
	(006)	not detected	29.062	0.8
	(007)	34.06 (34.27)[a]	34.039 (34.797)[b]	6.0
	(008)	not detected	39.099	1.0

[a]After 5 min UV irradiation. [b]Calculated for poly(MDO).

Figure 8. Several diffraction lines were observed at 2θ = 4.8, 9.6, 19.3, and 34.1°, and they can be assigned to the (001), (002), (004), and (007) planes, respectively (Table 1). The other weak diffractions were not detected under these conditions. Based on the XRD data, we assumed the tail-on-stacking of MDO on the KBr surface (Figure 8b). The *a*- and *b*-axes of the MDO crystals are parallel to the KBr surface in this tail-on-stacking form. However, we suspected that a series of diffraction lines was produced from the bent crystals with disturbed morphology shown in Figure 2b, and we further examined the crystal growth behavior of MDO. Figure 9 shows a change in the crystal growing pattern during the deposition of MDO on KBr with different deposition times. We have noticed that two types of crystal growth of MDO simultaneously occurred on the KBr surface during the initial stage of the deposition; one is crystals with a 100 nm height and nonuniform crystal shapes. This type of crystal favorably grows in a direction perpendicular to the substrate surface and

Figure 8. (a) Observed XRD profile and (b) tail-on-stacking structure for the MDO thin-film crystals deposited on KBr.

in a horizontal *b*-axis direction (type A). The other type of crystal growth resulted in the fabrication of 10-nm height crystals (type B). The latter crystals further grew in two-dimensional directions parallel to the substrate surface, leading to the formation of thin-plate crystals covering the whole
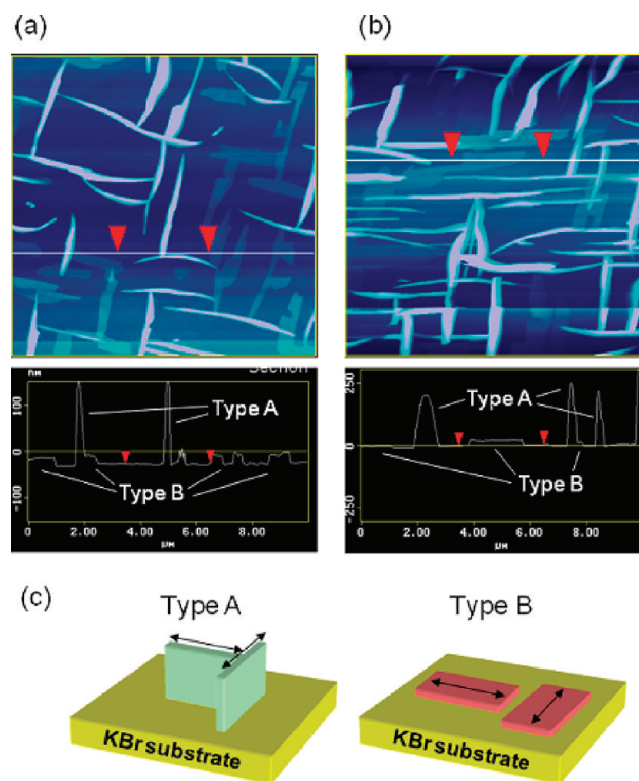
Figure 9. Two types of crystal growth of MDO observed in the AFM images of the MDO thin films fabricated by vapor deposition on the {001} plane of KBr. Area 10 μm × 10 μm. Deposition rate 0.02 nm/s. Deposition time (a) 10 and (b) 30 min. (c) Illustrative presentation of the crystal growth models for epitaxial crystal growth of MDO on KBr. The arrows indicate the direction of the *b*-axis of the crystals.

substrate surface. In fact, we isolated thin-plate crystals after deposition for several hours by dissolving the KBr substrate with water. Thus we have revealed that two types of the crystals were included in the AMF image of the thin-film crystals deposited on KBr. The X-ray diffractions shown in Figure 8 is caused by the type B crystals, but not the type A. The rate and habit in the crystal growth are quite consistent with the intermolecular interactions between the MDO molecules in both the crystals; i.e., intermolecular interaction is stronger between the MDO monomers arranged in the direction along the a- and b-axes because the molecules have contact in face-to-face and edge-to-edge fashions, respectively.

The epitaxial crystal growth on the KCl substrate is accounted for by the matching of the crystal lattice lengths of the MDO monomer and the substrates used, as summarized in Figure 10 and Table 2. The crystal lattice lengths of MDO are a
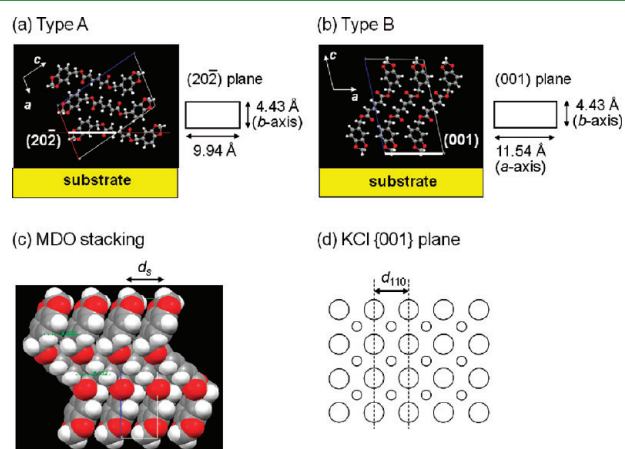
Figure 10. Parameters related to the epitaxial crystal growth of MDO on the {001} substrate surface. (a) (20-2) plane for the molecular stacking in type A, (b) (001) plane for the molecular stacking in type B, (c) the stacking of the MDO monomer molecules, and (d) d_{110} on the {001} plane of the KCl or KBr substrates. Large and small circles indicate halogen and potassium ions, respectively.

Table 2. Crystallographic Parameters and Misfit Values of Various Substrates

| substrate	a (Å)	d_{110} (Å)	misfit value[a] (%) along b-axis	orthogonal direction
KCl	6.293	4.449	−0.40	−0.7 (type A), +3.6 (type B)
KBr	6.596	4.664	+5.6 (−5.2)	+6.2 (type A), −1.0 (type B)
NaCl	5.640	3.988	−10.0	−0.3 (type A), −3.7 (type B)

[a]Misfit% = $(nd − md_{110})/nd \times 100$, where d is the unit length of the 2D lattice for epitaxial crystal growth (see also Figure 10), and n and m are any integer. One of the 2D lattice is equal to the b-axis of MDO (d_s = 4.43 Å) and the others are along the direction orthogonal to the b-axis. The unit lengths for the latters are 9.94 and 11.54 Å for the types A and B, respectively.

= 11.540, b = 4.4318, and c = 18.858 Å, where the b-axis is the monomer stacking direction, i.e., the fiber axis. For the KCl cubic crystal, the lattice length (a = 6.2931 Å) results in d_{110} = 4.45 Å, which agrees well with the d_s value of MDO (b = 4.43 Å). In contrast to the satisfactory matching of the lattice parameters in the case of KCl (the misfit was only −0.4%), the d_{110} values for KBr and NaCl are too large or small (d_{110} = 4.66 Å for KBr and d_{110} = 3.99 Å for NaCl). The misfit values were

±5 and −10% for KBr and NaCl, respectively. The negative misfit values are unfavorable for epitaxial crystal growth due to the compressed packing of the MDO molecules. The fast crystal growth in the b-axis direction significantly determines the occurrence of the epitaxial crystal growth processes, although mismatch in the other parameters between the MDO and the substrates should also be considered. The smaller misfit values are favored for the epitaxial growth and the positive misfit values are allowed than the negative one for the medium misfit values. As a result, the crystal growth in the type A was favored on KCl and the both type growths were possible on KBr in this study. In conclusion, the epitaxial crystal growth of MDO exclusively occurred on the KCl substrate according to the fashion of type A (edge-on-stacking), and the type-B crystal growth (tail-on-stacking) was preferred on the KBr substrate rather than the non-epitaxial type-A crystal growth. No epitaxial crystal growth occurred on NaCl.

Molecular Weight Control of Polymers. It is noted that the method described here may imply a possibility for the control of the molecular weight and distribution of the polymers as thin-film crystals deposited on substrates, because the molecular weight of the resulting polymers is closely related to the size of the crystal used for the polymerization,[57−59] i.e., the number of monomer molecules stacking along the polymerization axis in a crystal. We calculated the molecular weight of the polymers based on the size of the MDO crystals deposited on KCl with different deposition times, shown in Figures 2a, 3a, and 3b using the following assumptions. The topochemical polymerization perfectly occurs and produces polymers along the b-axis without any defect, i.e., the length of a polymer chain is equal to the length of the long axis of the crystals. The MDO crystals with orthogonally different directions independently undergo polymerization although the actual polymer shape is more complex, as shown in Figure 5. Actually, the length of the long axis (along the b-axis) was in a range of 1800−2000 nm, and the width of the crystals was also approximately constant, e.g., 200−300 nm. The height (thickness) of the crystals linearly increased to 100 nm during the deposition for 90 min (deposition rate was 0.02 nm/s). The calculated number-average molecular weight (M_n) and molecular weight distribution (M_w/M_n) values were M_n = 1.65, 1.49, and 1.51 × 10⁶ and M_w/M_n = 1.24, 1.23, and 1.19 for the thin-film poly(MDO) crystals by the deposition of 10, 30, and 90 min, respectively, followed by photopolymerization. These values were constant, independent of the height of the crystals, because the polymerization occurs along the b-axis direction. Experimental evidence for molecular weight determination by size-exclusion chromatography was not obtained because of the very small size of the samples in this study.

The molecular stacking structures observed in this study, both types A and B, included polymer chain alignment in parallel to the substrate surface. If we realize an alternative crystal growth of MDO, in which the b-axis perpendicularly exists toward the substrate surface, we can control the molecular weight of the resulting polymer by controlling the thickness of the thin-film crystals. Therefore, we investigated the possibility of perpendicular stacking of the MDO molecules and tested the alternative molecular stacking by CH−π interaction using alkyl-modified glass plates as the alternative substrate, as shown in Figure 11. The glass plate was cleansed by washing with acetone and 2-propanol followed by exposure to ozone for 40 min. The contact angle for water decreased from 33.0 ± 2.2° before cleansing to 25.7 ± 1.8° and 7.38 ±
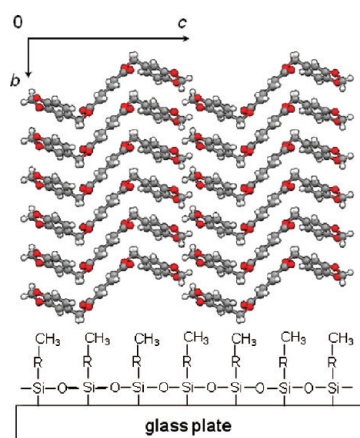
Figure 11. Face-on-stacking model for the MDO thin film deposited on an alkyl-modified glass plate.

0.97° after wet and ozone cleansing, respectively. The glass surface was then silanized by dipping in chloroform (50 mL) containing trichlorooctadecylsilane (5 μL) as the silane coupling agent for a determined time. The contact angle for water increased with an increase in the dipping time for the silanization and it reached a constant value (105 ± 1.2°) after 120 min reaction. The AFM images of the MDO thin films deposited on silanized glass plates are shown in Figure 12. The
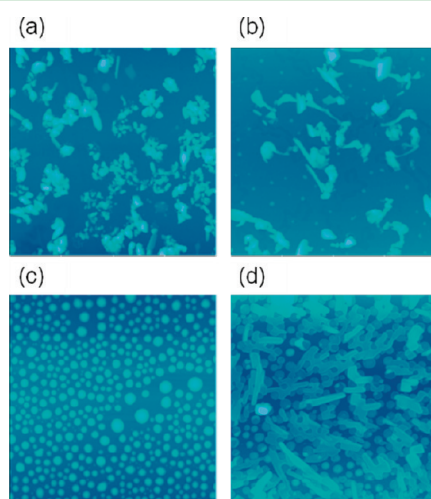
Figure 12. AFM images of the MDO thin films deposited on silanized glass plates. Alkylating agent: (a−c) trichlorooctadecylsilane and (d) trimethylmethoxysilane. The silanization time: (a) 5, (b) 15, (c) 120, and (d) 15 min. Deposition rate 0.02 mm/s, deposition time 30 min. Area 10 μm × 10 μm.

crystal growth with random arrangement was observed for the substrate with a shorter silanization time (5 and 15 min reactions), while the long-time silanization reaction resulted in the formation of islands consisting of liquid drops or amorphous solid. The use of other kinds of silane coupling agents, such as methyltrimethoxysilane, dimethyldimethoxysilane, and trimethylmethoxysilane, produced a similar unsuccessful result. No specific X-ray diffraction was obtained from the thin films deposited on alkyl-modified glass plates. We have concluded that the deposition of MDO with a face-on-stacking structure is difficult under the conditions used in this study. More sophisticated substrate surfaces and deposition

conditions are required in the alternative molecular stacking for controlling the molecular weight of the polymers. For example, any selected face of the single crystals of other muconate monomers or related compounds with similar lattice parameters is expected to induce crystal growth appropriate for the molecular weight control of the produced polymers.

CONCLUSION

We investigated the crystal growth of the MDO monomer thin films during vapor deposition for the control of polymer chain alignment by the subsequent solid-state photopolymerization. The epitaxial crystal growth of MDO on the {001} plane of a KCl single crystal was observed according to the molecular stacking fashion of type A (edge-on-stacking) under the condition that the crystal lattice lengths of MDO agreed well with the specific space distance of the substrate. The d_{110} value (4.45 Å) of the KCl cubic crystal was very close to the d_s value of MDO (4.43 Å). On the other hand, the d_{110} values for KBr and NaCl were 4.66 and 3.99 Å, respectively, resulting in the less controlled crystal growth of MDO on the substrates. The type-B crystal growth (tail-on-stacking) was preferred on the KBr substrate rather than the type-A crystal growth. No epitaxial crystal growth occurred on NaCl. The irradiation of polarized UV light on the MDO thin-film crystal produced highly regulated polymer alignment in a specific direction on the KCl substrate. The possibility for the molecular weight control of the polymers by the epitaxial vapor deposition of MDO was also discussed, but we concluded that the deposition of MDO with a face-on-stacking structure in a perpendicular direction to the substrate was difficult under the conditions used in this study.

AUTHOR INFORMATION

Corresponding Author
*Fax: +81-6-6605-2981. E-mail: matsumoto@a-chem.eng. osaka-cu.ac.jp.

Notes
The authors declare no competing financial interest.

ACKNOWLEDGMENTS

REFERENCES

(1) Matyjaszewski, K.; Davis, T. P., Eds. *Handbook of Radical Polymerization*; Wiley: New York, 2002.
(2) Hawker, C. J.; Wooley, K. L. *Science* **2005**, *309*, 1200−1205.
(3) Ouchi, M..; Terashima, T.; Sawamoto, M. *Chem. Rev.* **2009**, *109*, 4963−5050.
(4) Satoh, K.; Kamigaito, M. *Chem. Rev.* **2009**, *109*, 5120−5156.
(5) Wojtecki, R. J.; Meador, M. A.; Rowan, S. J. *Nat. Mater.* **2011**, *10*, 14−27.
(6) Ouchi, M.; Badi, N.; Lutz, J. -F.; Sawamoto, M. *Nat. Chem.* **2011**, *3*, 917−924.
(7) Wegner, G. *Z. Naturforsch* **1969**, *B24*, 824−832.
(8) Wegner, G. *Pure Appl. Chem.* **1977**, *49*, 443−454.
(9) Enkelmann, V. *Adv. Polym. Sci.* **1984**, *63*, 91−136.
(10) Sarkar, A.; Okada, S.; Matsuzawa, H.; Matsuda, H.; Nakanishi, H. *J. Mater. Chem.* **2000**, *10*, 819−828.

(11) Peng, H. −S.; Tang, J.; Pang, J. −B.; Chen, D. -Y.; Yang, L.; Ashbaugh, H. S.; Brinker, C. J.; Yang, Z. -Z.; Lu, Y. -F. *J. Am. Chem. Soc.* **2005**, *127*, 12782−12783.

(12) Ahn, D. J.; Kim., J. -M. *Acc. Chem. Res.* **2008**, *41*, 805−816.

(13) Lauher, J. W.; Fowler, F. W.; Goroff, N. S. *Acc. Chem. Res.* **2008**, *41*, 1215−1229.

(14) Okawa, Y.; Mandal, S. K.; Hu, C. -P.; Tateyama, Y.; Goedecker, S.; Tsukamoto, S.; Hasegawa, T.; Gimzewski, J. K.; Aono, M. *J. Am. Chem. Soc.* **2011**, *133*, 8227−8233.

(15) Shimogaki, T.; Matsumoto, A. *Macromolecules* **2011**, *44*, 3323−3327.

(16) Tieke, B. *Adv. Polym. Sci.* **1985**, *71*, 79−151.

(17) Matsumoto, A.; Matsumura, T.; Aoki, S. *J. Chem. Soc., Chem. Commun.* **1994**, 1389−1390.

(18) Matsumoto, A.; Odani, T. *Macromol. Rapid Commun.* **2001**, *22*, 1195−1215.

(19) Matsumoto, A. *Polym. J.* **2003**, *35*, 93−121.

(20) Matsumoto, A. *Top. Cur. Chem.* **2005**, *254*, 263−305.

(21) Hasegawa, M. *Adv. Phys. Org. Chem.* **1995**, *30*, 117−171.

(22) Coates, G. W.; Dunn, A. R.; Henling, L. M.; Ziller, J. W.; Lobkovsky, E. B.; Grubbs, R. H. *J. Am. Chem. Soc.* **1998**, *120*, 3641−3649.

(23) Ito, T.; Nomura, S.; Uno, T.; Kubo, M.; Sada, K.; Miyata, M. *Angew. Chem. Int. Ed.* **2002**, *41*, 4306.

(24) Takahashi, S.; Miura, H.; Kasai, H.; Okada, S.; Oikawa, H.; Nakanishi, H. *J. Am. Chem. Soc.* **2002**, *124*, 10944−10945.

(25) Itoh, T. *Polymer* **2005**, *46*, 6998−7017.

(26) Matsumoto, A.; Matsumura, T.; Aoki, S. *Macromolecules* **1996**, *9*, 423−432.

(27) Matsumoto, A.; Odani, T.; Chikada, M.; Sada, K.; Miyata, M. *J. Am. Chem. Soc.* **1999**, *121*, 11122−11129.

(28) Matsumoto, A.; Nagahama, S.; Odani, T. *J. Am. Chem. Soc.* **2000**, *122*, 9109−9119.

(29) Matsumoto, A.; Tanaka, T.; Tsubouchi, T.; Tashiro, K.; Saragai, S.; Nakamoto, S. *J. Am. Chem. Soc.* **2002**, *124*, 8891−8902.

(30) Ueno, T.; Furukawa, D.; Matsumoto, A. *Macromol. Chem. Phys.* **2008**, *209*, 357−369.

(31) Odani, T.; Okada, S.; Kabuto, C.; Kimura, T.; Shimada, S.; Matsuda, H.; Oikawa, H.; Matsumoto, A.; Nakanishi, H. *Cryst. Growth Des.* **2009**, *9*, 3481−3487.

(32) Atkinson, M. B. J; Halasz, I.; Bucar, D. -K.; Dinnebier, R. E.; Mariappan, S. V. S.; Sokolov, A. N.; MacGillivray, L. R. *Chem. Commun.* **2011**, *47*, 236−238.

(33) Lahav, M.; Schmidt, G. M. J. *J. Chem. Soc. B* **1967**, 312−317.

(34) Green, B. S.; Lahav, M.; Schmidt, G. M. J. *J. Chem. Soc. B* **1971**, 1552−1564.

(35) Mori, Y.; Matsumoto, A. *Cryst. Growth Des.* **2007**, *7*, 377−385.

(36) Odani, T.; Matsumoto, A.; Sada, K.; Miyata, M. *Chem. Commun.* **2001**, 2004−2005.

(37) Saltiel, J.; Krishna, T. S. R.; Clark, R. J. *J. Phys. Chem. A* **2006**, *110*, 1694−1697.

(38) Furukawa, D.; Kobatake, S.; Matsumoto, A. *Chem. Commun.* **2008**, 55−57.

(39) Nishizawa, N.; Furukawa, D.; Kobatake, S.; Matsumoto, A. *Cryst. Growth Des.* **2010**, *10*, 3203−3210.

(40) Matsumoto, A. *Molecular Nano Dynamics*; Fukumura, H., Irie, M., Iwasawa, Y., Masuhara, H., Uosaki, K., Eds.; Wiley-VCH: Weinheim, Germany, 2009; Vol. *2*, pp 459−486.

(41) Matsumoto, A.; Sada, K.; Tashiro, K.; Miyata, M.; Tsubouchi, T.; Tanaka, T.; Odani, T.; Nagahama, S.; Tanaka, T.; Inoue, K.; Saragai, S.; Nakamoto, S. *Angew. Chem. Int. Ed.* **2002**, *41*, 2502−2505.

(42) Matsumoto, A.; Furukawa, D.; Mori, Y.; Tanaka, T.; Oka, K. *Cryst. Growth Des.* **2007**, *7*, 1078−1085.

(43) Schimidt, G. M. J. *Pure Appl. Chem.* **1971**, *27*, 647−698.

(44) Ramamuuthy, V. *Photochemistry in Organized and Constrained Media*: VCH-Wiley: New York, 1991.

(45) Braga, D.; Grepioni, F., Eds., *Making Crystals by Design: Methods, Techniques and Applications*; Wiley-VCH: Weinheim, Germany, 2007.

(46) Pyun, J.; Matyjaszewski, K. *Chem. Mater.* **2001**, *13*, 3436−3448.

(47) Edmondson, S.; Osborne, V. L.; Huck, W. T. S. *Chem. Soc. Rev.* **2004**, *33*, 14−22.

(48) Hawker, C. J.; Russell, T. P. *MRS Bull.* **2005**, *30*, 952−966.

(49) Tsujii, Y.; Ohno, K.; Yamamoto, S.; Goto, A.; Fukuda, T. *Adv. Polym. Sci.* **2006**, *197*, 1−45.

(50) Huang, Z. Y.; Wang, P. C.; MacDiarmid, A. G.; Xia, Y. N.; Whitesides, G. *Langmuir* **1997**, *13*, 6480−6484.

(51) Malinauskas, A. *Polymer* **2001**, *42*, 3957−3972.

(52) Argun, A. A.; Aubert, P. H.; Thompson, B. C .; Schwendeman, I.; Gaupp, C. L.; Hwang, J.; Pinto, N. J.; Tanner, D. B.; MacDiarmid, A. G.; Reynolds, Jr. *Chem. Mater.* **2004**, *16*, 4401−4412.

(53) Alf, M. E.; Asatekin, A.; Barr, M. C.; Baxamusa, S. H.; Chelawat, H.; Ozaydin-Ince, G.; Petruczok, C. D.; Sreenivasan, R.; Tenhaeff, W. E.; Trujillo, N. J.; Vaddiraju, S.; Xu, J. J.; Gleason, K. K. *Adv. Mater.* **2010**, *22*, 1993−2027.

(54) Matsumoto, A.; Tanaka, T.; Oka, K. *Synthesis* **2005**, 1479−1480.

(55) Matsumoto, A.; Tanaka, T. *Mol. Cryst. Liq. Cryst.* **2005**, *440*, 215−222.

(56) Beard, A. R.; Hazell, S. J.; Mann, J.; Palmer, C. *J. Chem. Soc., Perkin 1* **1993**, 1235−1238.

(57) Iida, R.; Kamatani, H.; Kasai, H.; Okada, S.; Oikawa, H.; Matsuda, H.; Kakuta, A.; Nakanishi, H. *Mol. Cryst. Liq. Cryst.* **1995**, *267*, 95−100.

(58) Matsumoto, A.; Yokoi, K.; Aoki, S. *Polym. J.* **1998**, *30*, 361−363.

(59) Matsumoto, A.; Yokoi, K. *J. Polym. Sci., Part A: Polym. Chem.* **1998**, *36*, 3147−3155.